*Express Polymer Letters Vol.18, No.3 (2024) 309–325*
*Available online at www.expresspolymlett.com*
*https://doi.org/10.3144/expresspolymlett.2024.22*

*Research article*

# Influence of thermal degradation on the crystallization of poly(butylene terephthalate)

*Ahmed Nasr*[*], *Petr Svoboda*

Department of Polymer Engineering, Faculty of Technology, Tomas Bata, University in Zlin, Vavreckova 5669, 76001 Zlin, Czech Republic

*Received 4 September 2023; accepted in revised form 1 December 2023*

**Abstract.** Our work reveals a notable shift in the crystallization temperature ($T_c$) of poly(butylene terephthalate) (PBT) at which crystallization occurs due to exposure to prolonged thermal degradation at 270 °C in an environment of nitrogen gas. The initial $T_c$ of 193 °C undergoes a marked decrease, settling at 133 °C, which signifies a considerable 60 °C shift towards lower temperature ranges. This transition is discernible across three distinct degradation stages: an initial phase of increase, an intermediate phase characterized by a sharp decline, and a subsequent late stage of the degradation phase characterized by a more moderate decrease in $T_c$. Both crystallinity and crystallization kinetics consistently mirror this pattern, demonstrating an initial rise, a rapid subsequent drop, and a gradual decline in the late-stage period. Evident from the presence of two melting peaks, the research implies differing lamellar thicknesses. As the degradation progresses, the melting points of these peaks, denoted as $T_{m1}$ and $T_{m2}$, decline at 38 and 41 °C, respectively. Validation of the degradation-induced changes is provided by a small angle X-ray scattering (SAXS), which corroborates the observed decrease in the long period ($L$). A contextualization of the results against prior studies underscores analogous trends in the alteration of crystallization behaviour consequent to degradation.

***Keywords:*** *degradation, kinetics, crystallization, crystallinity, aromatic polyesters, PBT, differential scanning calorimetry, X-ray*

## 1. Introduction

The behaviour of polymers under various conditions of temperature and environmental exposure is paramount in material's science and engineering [1]. Polymer degradation, driven by thermal, mechanical or chemical factors, can change their macroscopic and molecular properties, influencing their overall performance and applicability [2]. Poly(butylene terephthalate) (PBT) is a high-performance thermoplastic polymer that has garnered significant attention within the domain of material's science and engineering due to its exceptional combination of mechanical, thermal, and electrical properties [3]. This semicrystalline polymer is derived from the condensation polymerization of terephthalic acid or dimethyl terephthalate with 1,4-butanediol. The resultant polymer exhibits a range of attributes that render it suitable for diverse industrial applications [4]. One of the most critical applications is polymer solar cells, such as Functional layers of inverted flexible perovskite solar cells and effective technologies for device commercialization, strain engineering toward High-Performance Formamidinium-Based Perovskite Solar Cells, high-performance inorganic perovskite solar cells and Mixed-Halide Inorganic Perovskite Solar Cells [5–7]. The alteration of PBT's crystallization behaviour under thermal degradation has emerged as a significant area of investigation, given its implications for material integrity and longevity [8].

The crystalline nature of polymers strongly influences their mechanical, thermal, and optical properties, rendering a comprehensive understanding of the crystallization process essential for informed material

[*]Corresponding author, e-mail: a_nasr@utb.cz

design and utilization [9]. Crystallization is a dynamic phenomenon involving transforming polymer chains from a disordered state to an ordered crystalline structure. This transformation is governed by a delicate interplay of many factors like temperature, molecular weight, processing conditions, and, notably, structural defects and degradation [10].

In recent years, researchers have increasingly turned their attention to the impact of thermal degradation on the crystallization kinetics and behaviour of polymers [11–14]. The structural changes induced by degradation can introduce defects, alter molecular weight distributions, and perturb chain mobility, all of which can influence crystallization dynamics. The scientific exploration of such changes advances our fundamental understanding of polymer behaviour. It offers valuable insights for practical applications, ranging from polymer processing and engineering to developing degradation-resistant materials. To our knowledge, no previous research has investigated the influence of thermal degradation on PBT's crystallization, which was carried out under a very long-time experiment.

This paper delves into the specific poly(butylene terephthalate) case and its crystallization behaviour under prolonged thermal degradation. By employing differential scanning calorimetry (DSC) and small-angle X-ray scattering (SAXS) techniques, the study examines the shifts in crystallization temperature ($T_c$), crystallinity, and crystallization kinetics as PBT undergoes various stages of thermal degradation. The investigation considers the complexities introduced by lamellar thickness variations and melting point shifts, shedding light on the intricate relationships between degradation-induced structural changes and crystallization tendencies.

Through a systematic analysis of the effects of thermal degradation on PBT's crystallization behaviour, this study contributes to a deeper comprehension of polymer degradation mechanisms and their repercussions. The insights garnered to have the potential to inform the design of polymers with enhanced durability and performance in the face of degradative conditions. Furthermore, by establishing parallels with prior research, this work aims to contextualize its findings within the broader landscape of polymer science, enriching the collective knowledge that underpins advancements in polymer engineering and material design.

## 2. Experimental method

The PBT variant used in this study, ARNITE T08-200, was supplied by DSM Company, headquartered in Genk, Belgium. PBT's molar mass is 34 000 g/mol. An illustration representing the molecular configuration of this PBT type is presented in Figure 1. For the small-angle X-ray scattering (SAXS) analysis, we used the Anton Paar SAXSpace instrument (Stuttgart, Germany). Samples were placed in the holder, and the distance between the sample and the detector was 268.5 mm. $CuK_\alpha$ was used with $U = 40$ kV, $I = 50$ mA, exposition time $t =$ 15 min. An imaging plate was used as a detector.

Before the degradation, the polymer was dried at 80 °C in a vacuum oven for 24 h. The degradation, crystallization and melting behaviour studies were performed in Mettler Toledo DSC 1 (Greifensee, Switzerland) machine under the nitrogen with a flow rate set at 200 ml/min. This DSC machine has some limits, *e.g.*, the maximum number of steps being 40. Initially, we did not know how long the experiment would last and how significant changes in crystallization and melting would happen. So at first, we chose the 50 min degradation steps. The 150 h degradation-crystallization experiment took 14 long experiments (each composed of 40 steps lasting about 15 h). The first-day experimental plan was slightly different from the following plans. Step #1: heating from 25 to 270 °C at heating rate 20 °C/min, step #2: isothermal annealing 1 min at 270 °C, step #3: cooling from 270 to 60 °C at cooling rate being 20 °C/min, step #4: heating from 60 to 270 °C at heating rate 20 °C/min, step #5: isothermal annealing 50 min at 270 °C, step #6: cooling from 270 to 60 °C at cooling rate 20 °C/min, step #7: heating from 60 to 270 °C at heating rate 20 °C/min, step #8: isothermal annealing 50 min at 270 °C, step #9: cooling from 270 to 60 °C at cooling rate 20 °C/min, … continued similarly till step 40.

The first-day plan contained the initial 1 min annealing time, while the following days included only 50 min annealing periods. The 1 min period was just for the first crystallization reference point, but then it was not needed.

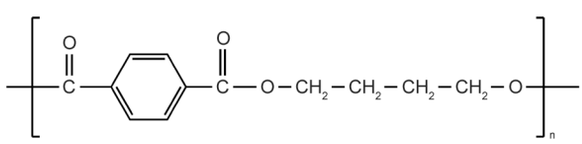


**Figure 1.** Chemical structure of PBT.

Heating steps were: 1, 4, 7, 10, 13, 16, 19, 22, 25, 28, 31, 34, 37 and 40, all were done at 20 °C/min heating rate. Cooling steps were: 3, 6, 9, 12, 15, 18, 21, 24, 27, 30, 33, 36 and 39, all were done at 20 °C/min cooling rate. The program was slightly modified the following days, and all the isothermal annealing steps at 270 °C lasted 50 min. The crystallinity percentage of PBT was calculated at a heat of fusion of 142 J/g for 100% crystalline PBT [15]. The heating and cooling rate 20 °C/min is rather common in literature even though some researchers use 10 °C/min. The higher rate has an advantage of faster processing time, and the degradation during the heating and cooling is smaller. The isothermal annealing was initially only 1 min, but there was a 50 min time period, so we got change in crystallization in precise time intervals.

Relative crystallinity was calculated in Excel as cumulative heat flow that was recalculated then to be in range 0–1.

Measurement of molecular weight was done using gel permeation chromatography (GPC). PBT samples were dissolved in Hexafluoroisopropanol (HFiP) (Sigma-Aldrich s.r.o., Prague, Czech Republic) containing 0.1 M potassium trifluoride (Sigma-Aldrich s.r.o., Prague, Czech Republic) at a concentration of 2.0 g/L. The injection volume was 100 µL, and the analysis temperature was set to 40 °C. The measurements were carried out utilizing an e2695 GPC instrument (Waters GmbH, Vienna, Austria). The reported molar masses were expressed in poly(methyl methacrylate) (PMMA) (Sigma-Aldrich s.r.o., Prague, Czech Republic) equivalents.

## 3. Results and discussions

The change of molar mass during degradation at 270 °C in nitrogen atmosphere is illustrated in Figure 2. Initially (during few several hours) the decrease is rather steep. After about 7 h the decrease in $M_n$ is rather moderate. These results agree well with Passalacqua *et al*. [14] who studied the influence of thermal degradation of PBT on molar mass change in $N_2$ at temperatures 240, 250, 260, 280 and 300 °C.

Mechanisms of thermal degradation of PBT were well described by several authors [11, 12, 16–19] and included random chain-scission, cross-linking, cyclization and desertification. One possible mechanism of PBT degradation is depicted in Figure 3. Some of the degradation products are solid or liquid, and some are gas. The gas products' escape from the sample and the weight loss was detected and recorded during the 150 h degradation experiment.

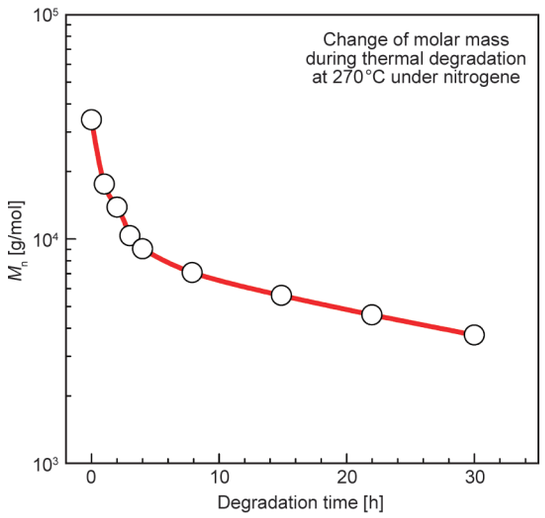


**Figure 2.** The influence of degradation time on the molar mass of PBT.

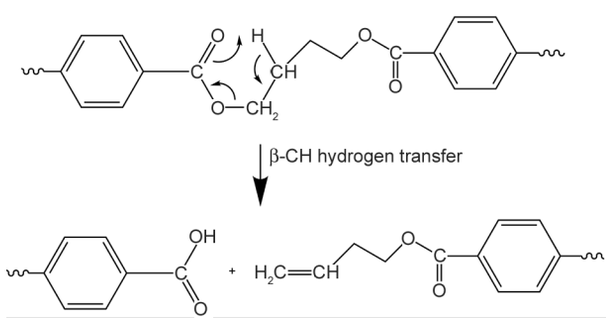


**Figure 3.** One possible mechanism of PBT degradation.

At the beginning of the degradation experiment, we observed an interesting increase in the position of crystallization temperature $T_c$ from 182 to 189 °C, peak height increased from about 2.1 to 3.1 W/g; it changed from broad to narrower – see Figure 4. After integration, the relative crystallinity curves were obtained, called 'S-curve', and then the slope at the inflection point was evaluated, which relates to the maximum in crystallization kinetics. The slope (or the crystallization kinetics) has significantly increased from 0.035 to 0.044 (Table 1). The kinetics were also evaluated with the help of a modified Avrami equation (for nonisothermal crystallization). Our results in the initial degradation period agree well with other researchers [20, 21].

Avrami model [22] provides a mathematical framework to analyze the fraction of crystalline material as a function of time, which is described in Equation (1):

$$\ln\left[-\ln\left(1-X_t\right)\right] = \ln k + n\ln t \tag{1}$$

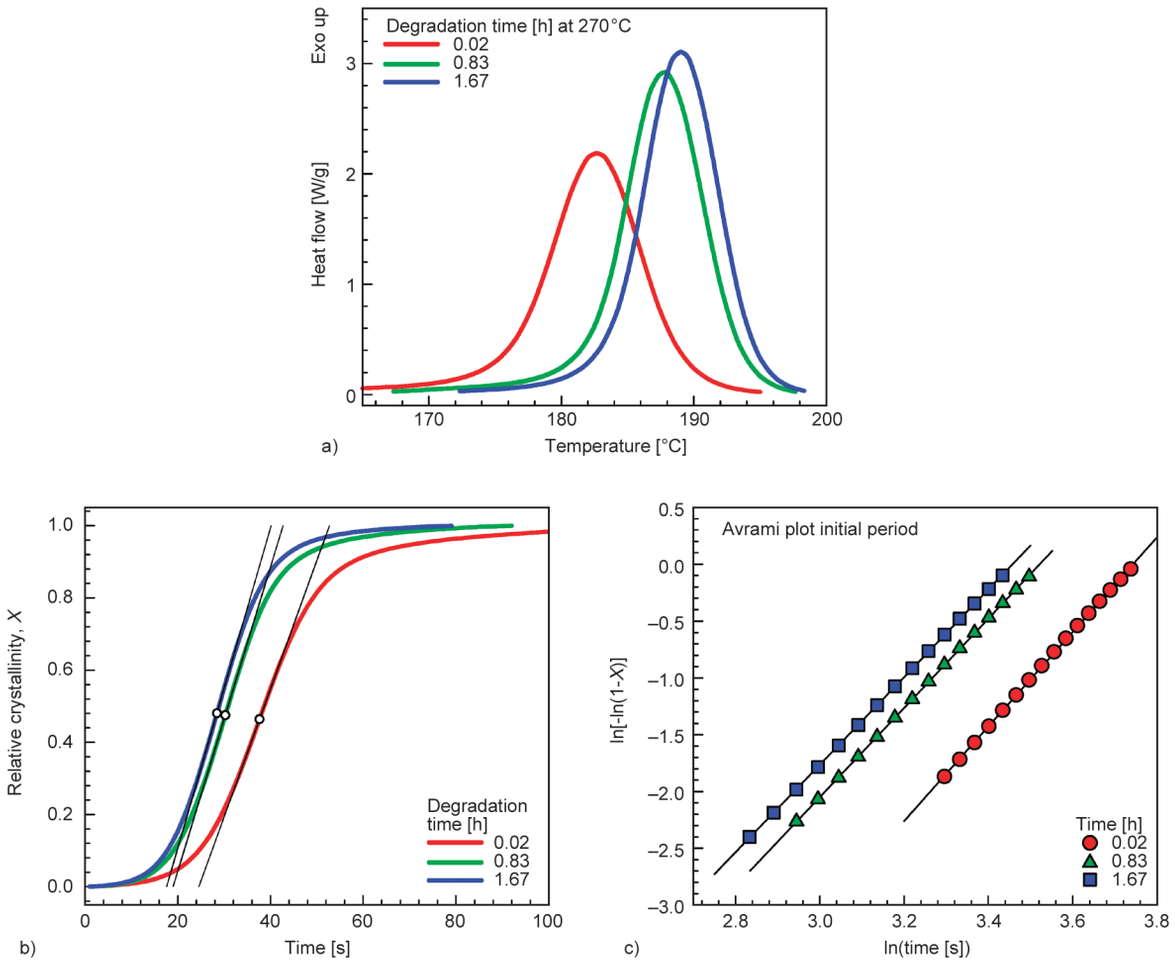


**Figure 4.** Nonisothermal crystallization measured by DSC at 20 °C/min cooling rate – initial period, a) heat flow, b) relative crystallinity, c) Avrami plot.

**Table 1.** PBT properties.

| Property | PBT DSM Arnite T08-200 | |
|---|---|---|
| Melt temperature (10 °C/min) | 225 °C | ISO 11357-1/-3) |
| Tensile modulus | 2550 MPa | (ISO 527-1/-2) |
| Charpy notched impact strength | 6 kJ/m$^2$ at 23 °C | (ISO 179/1eA) |
| Density | 1300 kg/m$^3$ | (ISO 1183) |
| MFI at 250 °C, load 2.16 kg | 13 g/10 min | (ISO 1133) |

where $n$ is Avrami exponent, $k$ Avrami rate constant, and $X_t$ is the relative crystallinity of polymer at time $t$.

Initially, degradation of PBT caused increased $T_c$. It seems that at a certain range of molecular weight the decrease in $M_w$ causes easier crystallization that is demonstrated by the $T_c$ shift towards higher temperature. Ergoz *et al*. [23] have shown (for polyethylene) that in the lowest range of $M_w$ the decrease in $M_w$ causes a decrease in crystallization rate. At the same time, at the higher range of $M_w$ the decrease in $M_w$ causes an increase in crystallization rate and there is also a $M_w$ range when the decrease in $M_w$ has almost no effect on crystallization rate. Chen *et al*. [24] had the same poly(ε-caprolactone) conclusion.

Rangari and Vasanthan [20] showed that PLA sample had $T_c$ before degradation at 89 °C, and after 10 days of degradation, the $T_c$ was 96 °C.

They explained the $T_c$ increase in this way. The $T_g$ and $T_c$ depend primarily on chain flexibility, molecular weight, and cross-linking, suggesting that segmental interaction increased as a function of degradation time for the PLA film.

Chen *et al*. [25] observed an increase in $T_c$ with decreasing molecular weight of poly(trimethylene terephthalate) (PTT). Their PTT samples had $M_\eta$ 12800, 17600, 21200 and 28000 g/mol; corresponding $T_c$ was 185.2, 182.0, 180.0 and 178.6 °C.

Unlike the initial crystallization period, the intermediate period shows a decrease in the crystallization peak position $T_c$ – see Figure 5. In the time range 5–38 h, the $T_c$ has changed from 187 to 149 °C (a significant 38 °C decrease), and the peak height decreased initially from 3.2 to 2.3 W/g (time 5–20 h),

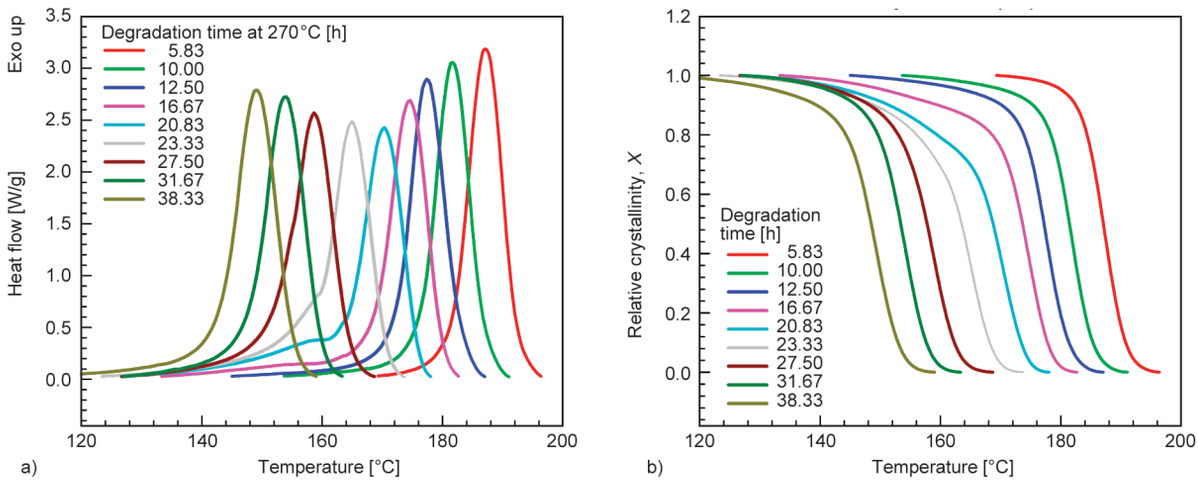


**Figure 5.** Nonisothermal crystallization measured by DSC at 20 °C/min cooling rate – intermediate period. Normalized to sample size, a) heat flow, b) relative crystallinity.

and then it remained approximately constant (time 20–38 h). Our data agree well with other researchers. Rabello and White [26] observed decreased $T_c$ for photodegraded polypropylene; initially, the $T_c$ was 115 °C, and after 24 weeks of photodegradation, it was 108 °C. Muthuraj *et al*. [27] studied poly(butylene succinate) (PBS) and observed a decrease in $T_c$ after degradation – 30 days of continuous conditioning at 50 °C and 90% relative humidity (*RH*). Initially, the PBS sample had $T_c$ 92 °C and after degradation, it was 77 °C. Avela *et al*. [28] observed a lower $T_c$ for polypropylene with lower molecular weight.

Wang *et al*. [29] observed a decreased $T_c$ for poly (trimethylene terephthalate) samples with lower molecular weight. The reported $M_n$ values were 67 000, 27 000, 23 000 and 13 000 g/mol. The respected $T_c$ values were approximately 182, 178, 173 and 163 °C.

Xu and Shi [30] studied the crystallization kinetics of silsesquioxane-based hybrid star poly(ε-caprolactone) and found a lower position of crystallization peak $T_p$ for polymers with lower molecular weight. For example, the samples with $M_n$ being 269 840 and 30 368 g/mol had at cooling rate 10 °C/min the position of crystallization peak $T_p$ 33.9 and 19.5 °C respectively.

Figure 6 illustrates the late degradation stage's influence on nonisothermal crystallization. The time frame for degradation was 38–150 h. The prolonged degradation at 270 °C is taking a toll on the polymer sample. We observed a further decrease in $T_c$ (from 149 to 132 °C), but this time, the peaks became gradually lower and broader, suggesting changes in crystallinity and crystallization kinetics. The decrease in peak height was quite tremendous (from 2.78 to 0.70 W/g). The crystallization kinetics expressed as the slope at the inflection point decreased from 0.035 to 0.013 (as shown in Table 2).

Samperi *et al*. [11] describe in detail the thermal degradation of poly(butylene terephthalate) at the processing temperature, possible mechanisms of degradation, and many degradation products.

Figure 7 illustrates the influence of cooling rate on nonisothermal crystallization after 15 h of degradation. At cooling rate 25 °C/min, the peak position is at the lowest value (175 °C), and there is a slight shoulder at 183 °C suggesting crystallization of two different lamellae at two different crystallization rates. The real presence of two crystallization peaks becomes even more pronounced at lower cooling rates. At a cooling rate 5 °C/min, there is a clear presence of two peaks at 184.8 and 189.4 °C. This result corresponds well to the presence of two melting peaks shown in Figure 13. Seo *et al*. [31] described this phenomenon in terms of primary and secondary crystallization kinetics. They used Avrami and Nakamura's dual models to describe such crystallization behavior. We have followed their example and obtained dual Avrami and Nakamura parameters. They are listed in Table 3 and dual Nakamura parameters are also shown in Figure 10. Initially (at higher temperatures), the crystallization is slower, reflected both by lower Avrami $k_1$ parameter and lower Nakamura $K_1$ parameter. This is followed by much faster crystallization at lower temperatures, which is reflected by much higher Avrami $k_2$ and Nakamura $K_2$ parameters.

Our results correspond well with Rabello and White [26], who also observed decreased crystallization

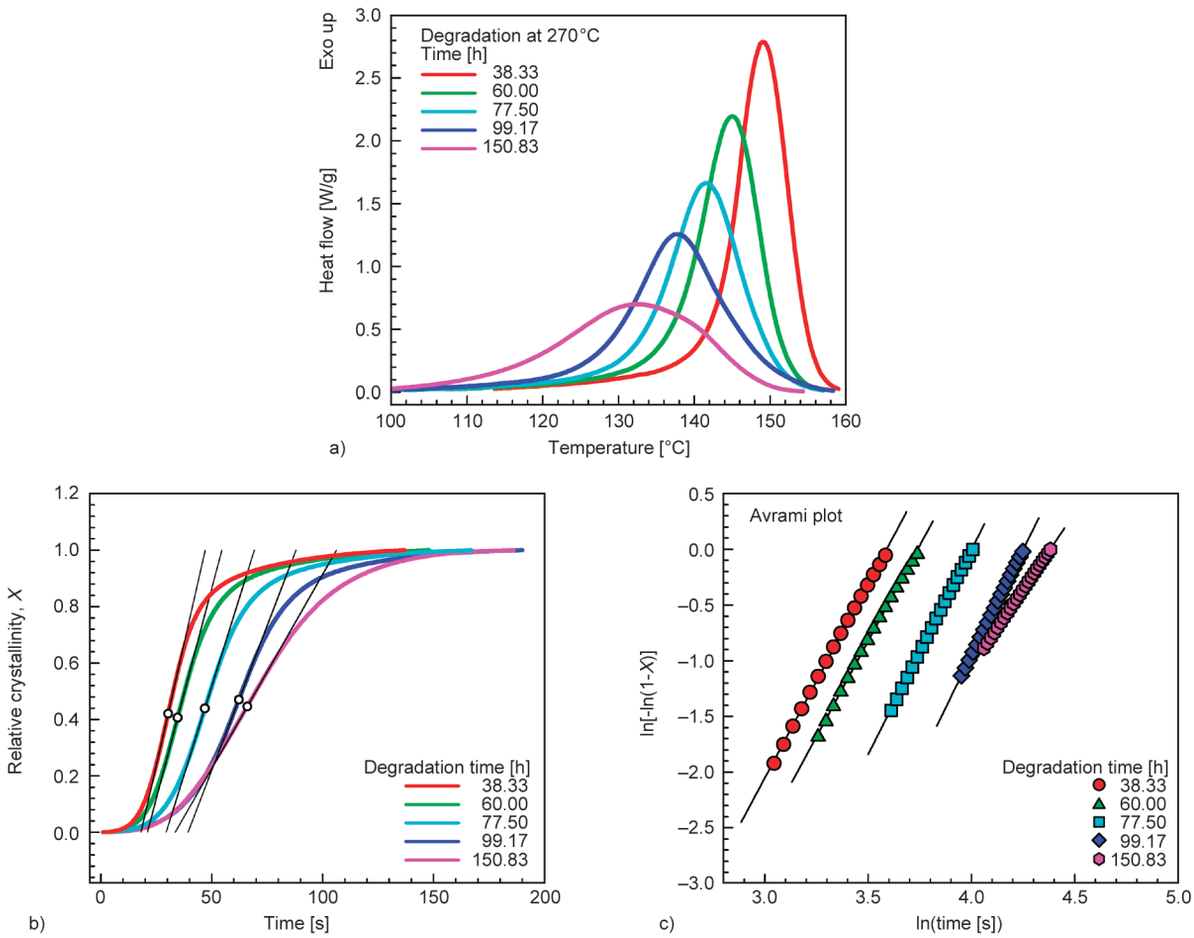


**Figure 6.** Nonisothermal crystallization measured by DSC at 20 °C/min cooling rate – late stage. Normalized to sample size, a) heat flow, b) relative crystallinity, c) Avrami plot.

**Table 2.** Crystallization kinetics parameters as a function of degradation time at 270 °C: half time of crystallization $\tau_{1/2}$, reciprocal half-time of crystallization $\tau_{1/2}^{-1}$, Nakamura parameter $K = k^{1/n}$, the slope at the inflection point.

| Time [h] | $\tau_{1/2}$ [s] | $\tau_{1/2}^{-1}$ [s$^{-1}$] | $K = k^{1/n}$ | Slope [s$^{-1}$] |
|---|---|---|---|---|
| 0.02 | 38.63 | 0.02589 | 0.02330 | 0.03545 |
| 0.83 | 30.84 | 0.03243 | 0.02907 | 0.04219 |
| 1.67 | 28.86 | 0.03465 | 0.03105 | 0.04437 |
| 5.83 | 28.86 | 0.03464 | 0.03091 | 0.04379 |
| 10.00 | 29.74 | 0.03362 | 0.02973 | 0.04131 |
| 12.50 | 30.43 | 0.03286 | 0.02906 | 0.03968 |
| 16.67 | 28.14 | 0.03553 | 0.03032 | 0.03943 |
| 20.83 | 28.78 | 0.03474 | 0.02853 | 0.03902 |
| 23.33 | 31.43 | 0.03182 | 0.02668 | 0.03771 |
| 27.50 | 33.64 | 0.02973 | 0.02576 | 0.03751 |
| 31.67 | 30.88 | 0.03238 | 0.02835 | 0.03621 |
| 38.33 | 32.56 | 0.03071 | 0.02683 | 0.03459 |
| 60.00 | 37.73 | 0.02650 | 0.02324 | 0.02978 |
| 77.50 | 49.32 | 0.02027 | 0.01812 | 0.02515 |
| 99.17 | 63.62 | 0.01572 | 0.01418 | 0.02054 |
| 150.83 | 69.91 | 0.01430 | 0.01250 | 0.01377 |

kinetics for photodegraded polypropylene and Fraïsse *et al*. [32], who observed decreased crystallization kinetics for photo and thermo-aged poly(ethylene oxide). Ergoz *et al*. [23] found a tremendous decrease in the crystallization kinetics of linear polyethylene when $M_w$ decreased from 20 000 to 5000 g/mol.

Figure 8 illustrates the change in the position of crystallization peak $T_c$ and crystallinity $X$ as a function of degradation time. The change in $T_c$ position can be divided into three time-ranges. The $T_c$ increases sharply in the initial period (0.02–1.67 h). The $T_c$ decreases sharply during the intermediate time range (3.3–31.7 h). Finally, in the late stage of degradation (45–150 h), the decrease of $T_c$ is relatively moderate. The crystallinity had to be corrected by the measurement of weight loss. We can detect initial increase (0–5 h) followed by approximately constant value (5–60 h), then there is a decrease (60–100 h) and finally almost constant value (100–150 h).

Our initial increase in $T_c$ corresponds well with Rangari and Vasanthan [20], who studied crystallization after and enzymatic degradation of poly(L-lactic

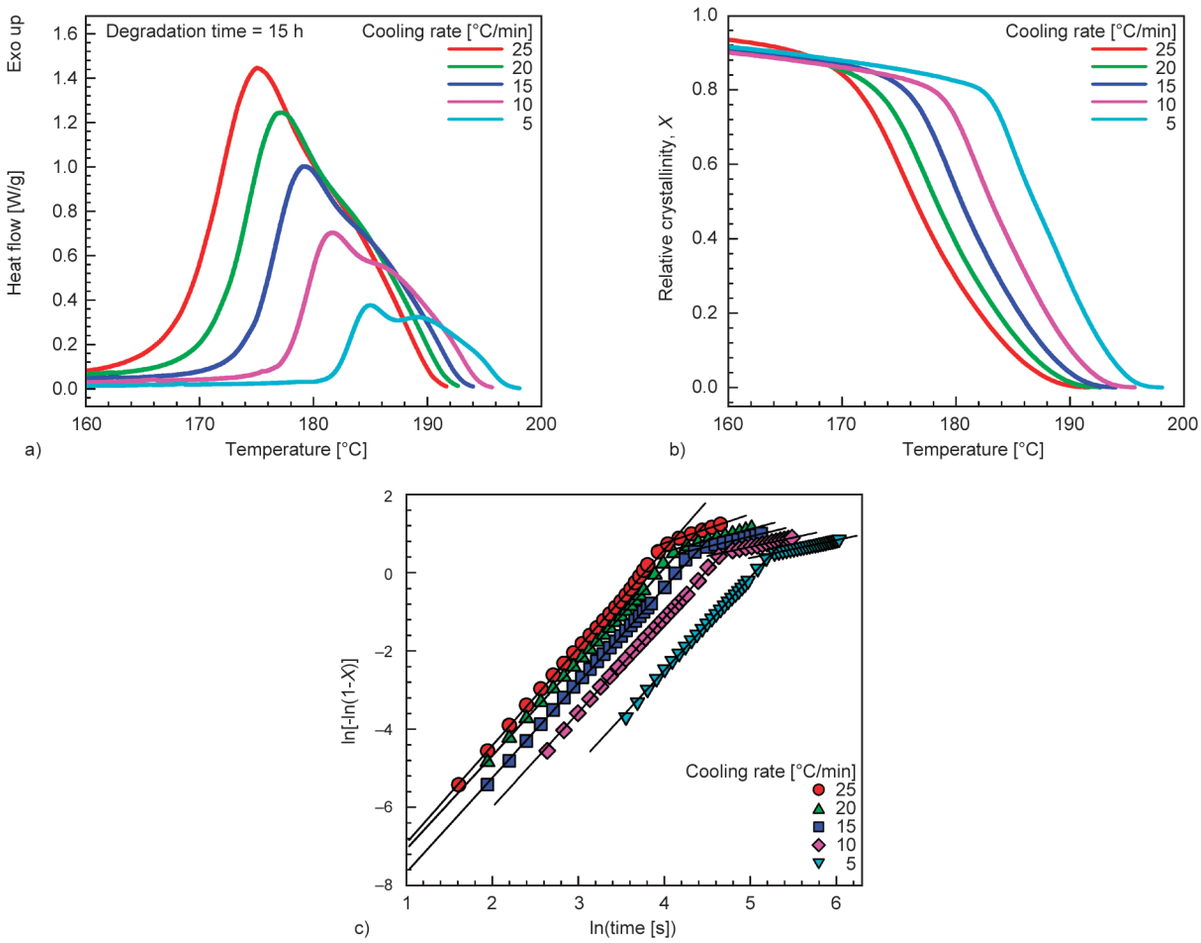


**Figure 7.** Nonisothermal DSC experiment at various cooling rates. Evaluation of dual Avrami parameters for degradation time 15 h: a) heat flow, b) relative crystallinity, c) Avrami plot.

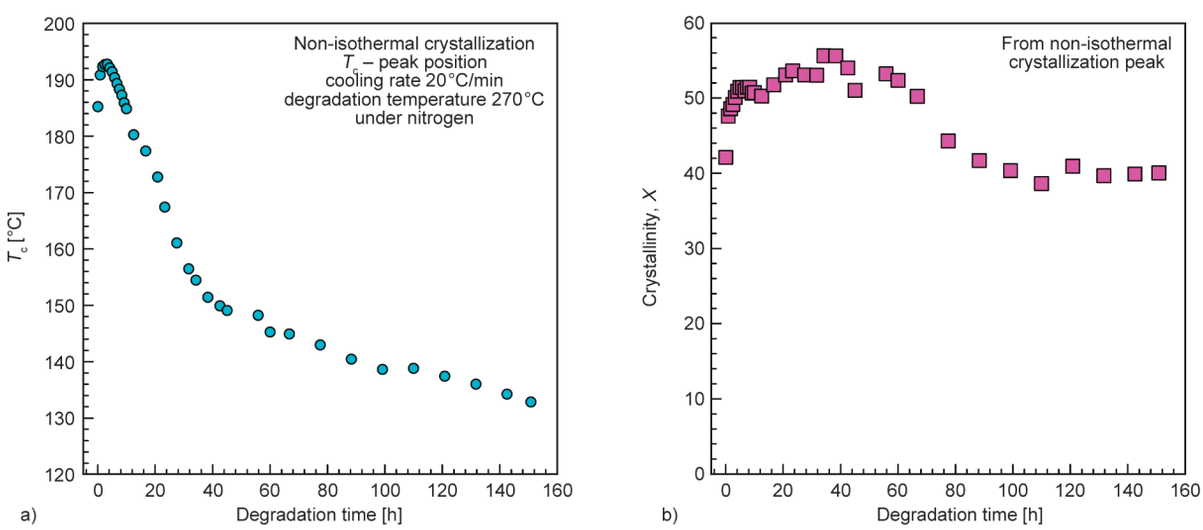


**Figure 8.** a) Crystallization peak position $T_c$ and b) relative crystallinity $X$ as a function of degradation time at 270 °C. Measured by DSC at 20 °C/min cooling rate. Normalized to sample size.

acid) (PLLA) films. In their case, the $T_c$ has increased from 89 to 96 °C after 10 days of degradation, and crystallinity has increased from 19.7 to 23.2% [20]. Our initial increase in crystallinity corresponds also well with Tsuji *et al*. [33] who studied the hydrolytic degradation of poly(L-lactic acid) and found an increase in crystallinity during the degradation.

Wang *et al*. [29] studied the effect of molecular weight on crystallization of poly(trimethylene terephthalate). They had samples with $M_n$ being 67 000,

27 000, 23 000 and 13 000 g/mol. Corresponding crystallinities were 35, 36, 30 and 29%. Thus, our results are in good agreement with Wang *et al*. [29], they also observed initial increase in crystallinity followed by a decrease with decreasing $M_n$.

Figure 9 and Table 2 illustrate the influence of thermal degradation on (Figure 9a) the slope at the inflection point, (Figure 9b) the Nakamura K parameter and (Figure 9c) the reciprocal of crystallization half-time ($\tau_{1/2}^{-1}$). The crystallization kinetics is highly influenced by the degradation time.

As it can be seen, a parallel trend emerges, consistent with the alterations observed in crystallinity and peak position (see Figure 8).

Initially introduced in 1973, the Nakamura model [34] is a firmly established paradigm for characterizing nonisothermal polymer crystallization. Rooted in this model is a comprehensive consideration of both temperature and the degree of crystallization within the polymer, further encompassing the crystallization kinetics delineated by the Avrami equation (Equation (2)):

$$K(T) = k(T)^{\frac{1}{n}} \tag{2}$$

where $n$ and $k$ are Avrami parameters, required to calculate the Nakamura $K$ constant.

The complex effect of molecular weight on crystallization was illustrated by several researchers [23, 24, 35, 36]. They showed a hill-like shape of the crystallization kinetics as a function of $M_w$. Our results are in good agreement with these observations. Initially the crystallization kinetics increases. This result follows the trend shown by Wu *et al*. [37] who reported increase in crystallization kinetics for samples of polyethylene with $M_n$ being 18 360, 17 150 and 16 540 g/mol and the $\tau_{1/2}$ for these samples at 122 °C was 5.6, 4.8 and 3.7 min, clearly with

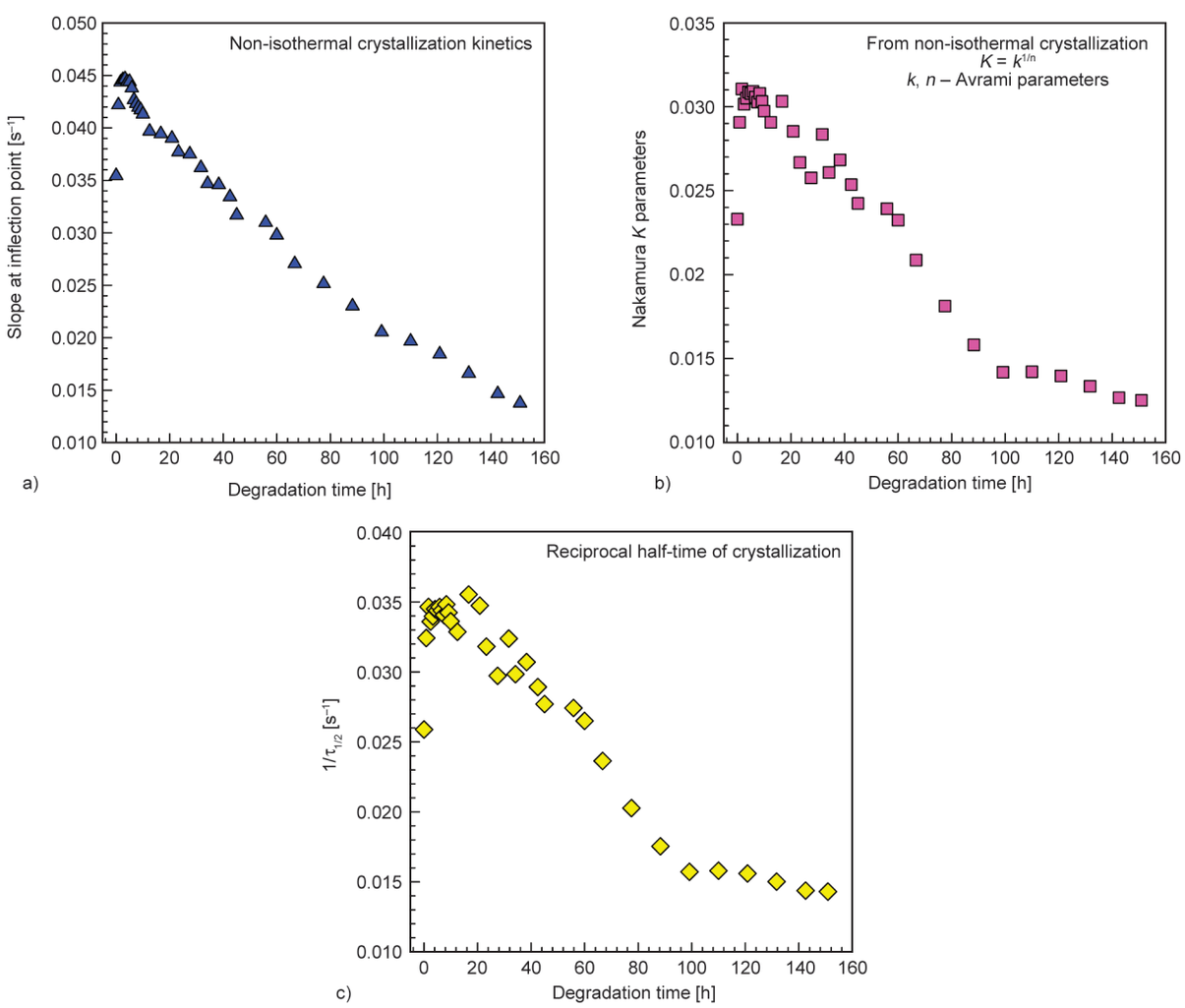


**Figure 9.** Crystallization kinetics from DSC nonisothermal experiment expressed by: a) slope at the inflection point of the S-curve, b) Nakamura $K$ parameter, c) reciprocal crystallization half-time $\tau_{1/2}^{-1}$.

a decrease in $M_n$ the isothermal crystallization was faster.

In certain degradation time range, there seems to be almost no change (or very little) in crystallization kinetics expressed by Nakamura $K$ parameter (Figure 9b) and by reciprocal half time of crystallization (Figure 9c). This result is comparable *e.g.* to Galante *et al*. [38] and to Isayev and Catignani [39]. Galante *et al*. [38] studied metallocene type polypropylenes, $M_w$ range was $68 \cdot 10^3$–$288 \cdot 10^3$ g/mol, the crystallization rate was assessed as $1/\tau_{0.2}$ (inverse time to attain 20% of the total transformation). They concluded that crystallization rates for given crystallization temperature were essentially same for all studied polymers or in other words, there was no influence of $M_w$ on crystallization kinetics. Isayev and Catignani [39] studied polypropylene with $M_w$ in range $70 \cdot 10^3$–$670 \cdot 10^3$ g/mol by optical microscopy. They concluded that above a certain value of molar mass, the linear growth rate of spherulites is independent of $M_w$.

Our results also show that the crystallization kinetics is decreasing in a certain degradation time range. These results correspond well with Ergoz *et al*. [23], who showed an enormous decrease in the crystallization kinetics of polyethylene when the $M_\eta$ was decreased from 20 000 to 4200 g/mol.

Ozawa model [40] takes into consideration the impacts of the distribution of crystal size on the non-isothermal crystallization kinetics, as depicted in Equation (3):

$$X = 1 - \exp\left[\frac{-K(T)}{\phi^m}\right] \tag{3}$$

where $X$ symbolizes crystallinity, $m$ is the Ozawa parameter illustrating the nucleation and growth of crystals, $K$ is Ozawa's rate constant, and $\phi$ represents the cooling rate. Equation (4) is obtained by applying double logarithms to Equation (3):

$$\log[-\ln(1-X)] = \log K(T) - m\log\phi \tag{4}$$

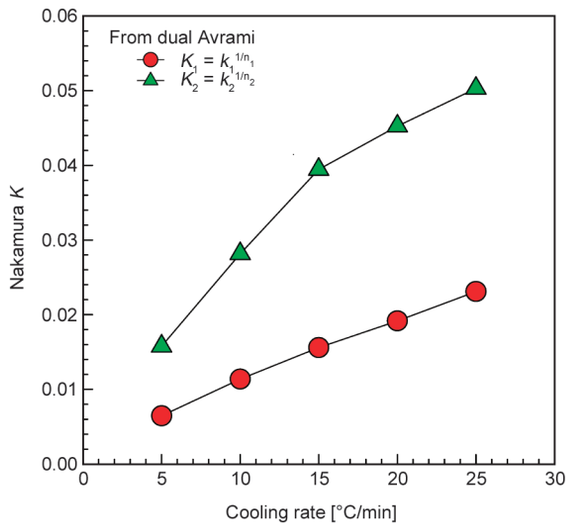


**Figure 10.** Nakamura $K_1$ and $K_2$ parameters from dual Avrami plots for degradation time 15 h.

Figure 11 shows the Ozawa cooling function at different degradation times by applying various cooling rates (15, 20 and 25 °C/min). As can be seen, the Ozawa cooling function moves towards the lower temperatures with increasing degradation time. The shift of the cooling function towards the lower temperatures corresponds well to the shift in $T_c$ illustrated in Figure 11.

Additionally, an excellent linear relationship between $\log[-\ln(1 - X(t))]$ and $\log\phi$ is obtained at different cooling rates. This linear relationship confirms the validity of the Ozawa model. To obtain a nice linear relationship, we had to choose similar (or not very far) cooling rates (15, 20 and 25 °C/min). Ozawa himself used rates 1, 2 and 4 °C/min and observed a nice linear relationship. Some researchers try to use a much wider range of cooling rates, such as 1–50 °C/min and fail to get a nice linear relationship.

Figure 12 shows the melting behaviour at various heating rates. At lower degradation times, we can see a peak for cold crystallization that is typical for polyesters; however, at longer degradation times, there is no cold crystallization peak, and we can clearly see

**Table 3.** Dual Avrami and Nakamura parameters for degradation time = 15 h.

| Cooling rate [°C/min] | Avrami parameters | | Nakamura parameter | Avrami parameters | | Nakamura parameter |
|---|---|---|---|---|---|---|
| | $n_1$ | $k_1$ | $K_1 = k_1^{1/n_1}$ | $n_2$ | $k_2$ | $K_2 = k_2^{1/n_2}$ |
| 25 | 2.49877 | $8.14287 \cdot 10^{-5}$ | 0.0230944 | 0.744120 | 0.108105 | 0.0503054 |
| 20 | 2.39468 | $7.70817 \cdot 10^{-5}$ | 0.0191613 | 0.585162 | 0.163427 | 0.0452510 |
| 15 | 2.42770 | $4.09666 \cdot 10^{-5}$ | 0.0155849 | 0.523750 | 0.183972 | 0.0394625 |
| 10 | 2.42114 | $1.96273 \cdot 10^{-5}$ | 0.0113715 | 0.462041 | 0.192122 | 0.0281474 |
| 5 | 2.40819 | $5.32581 \cdot 10^{-6}$ | 0.0064586 | 0.447950 | 0.155924 | 0.0157857 |

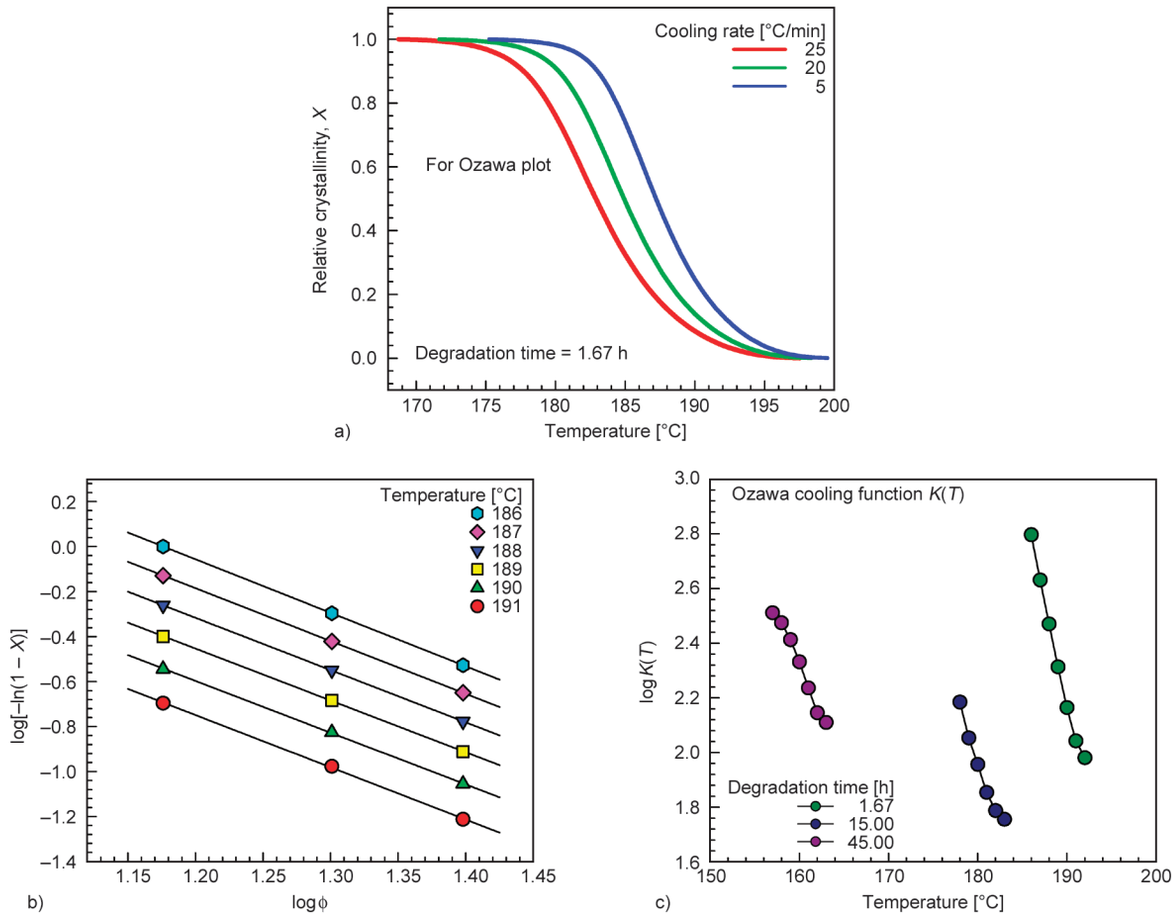


**Figure 11.** a) Influence of cooling rate on the relative crystallinity, b) Ozawa plot for different cooling rates for degradation time 1.67 h, c) Ozawa cooling function.

two melting peaks. A lower heating rate makes better visibility of two melting peaks.

Several authors have reported a change in melting point $T_m$ towards lower values during degradation [26, 33, 41, 42]. Figure 13 shows the change in melting temperature by the thermal degradation at 270 °C. Increasing the degradation time, the peak shifts towards the lower temperatures and then two melting points appear ($T_{m1}$ and $T_{m2}$). The melting peak has two maxima, which could be a result of primary/secondary crystallization kinetics that could be modelled by a dual Avrami model [31].

Figure 14 and Table 4 confirm this effect of thermal degradation on PBT's melting temperature and

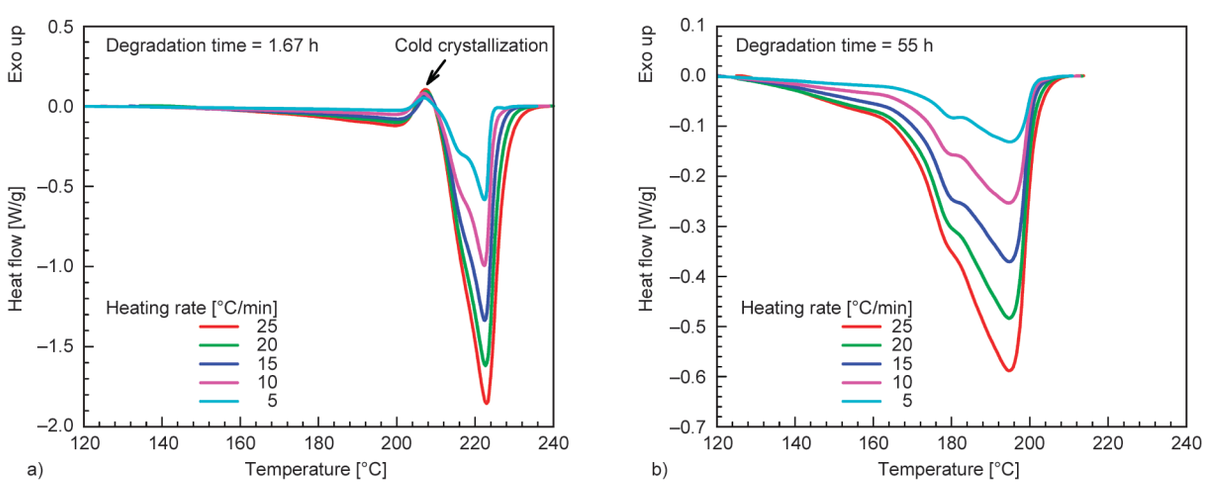


**Figure 12.** Melting behaviour at various heating rates: a) degradation time = 1.67 h, b) degradation time = 50 h.

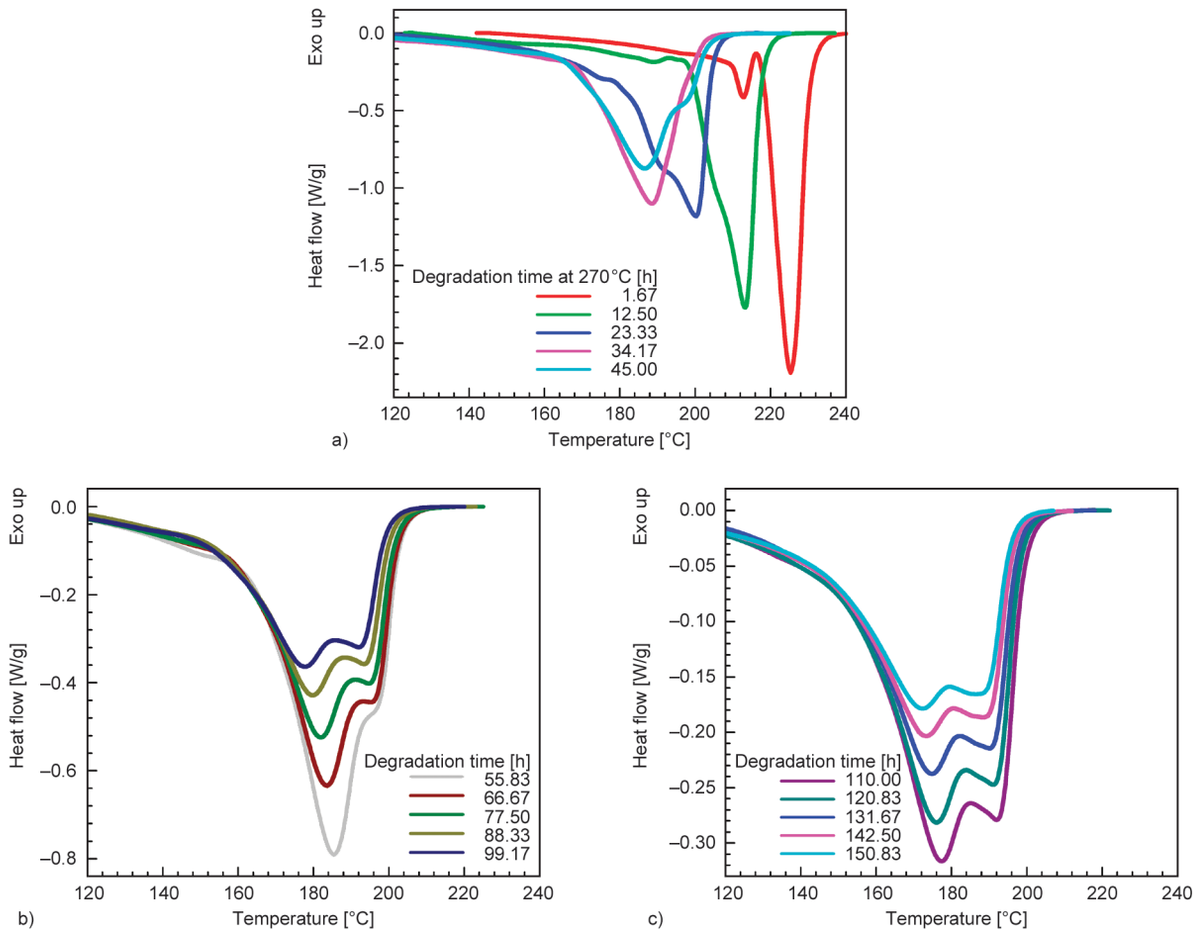


**Figure 13.** DSC results at heating rate 20 °C/min: change in melting behaviour by the thermal degradation at 270 °C, a) intermediate stage, b) first half of late stage, c) second half of late stage.

crystallinity. Initially (0–20 h), the change in $T_m$ for PBT is enormous, then from 20 to 150 h the change is relatively moderate. The presence of two melting peaks is clear.

The crystallinity curve (from melting during the heating step) was corrected again for the weight loss during the extended degradation time. There is a significant increase in crystallinity for samples degraded 1.67 to 34.17 h. Our initial increase in $T_c$ corresponds well with Rangari and Vasanthan [20] and Tsuji *et al*. [33]. From 34.17 to 88.33 h there is a rather large decrease in crystallinity. Finally, from

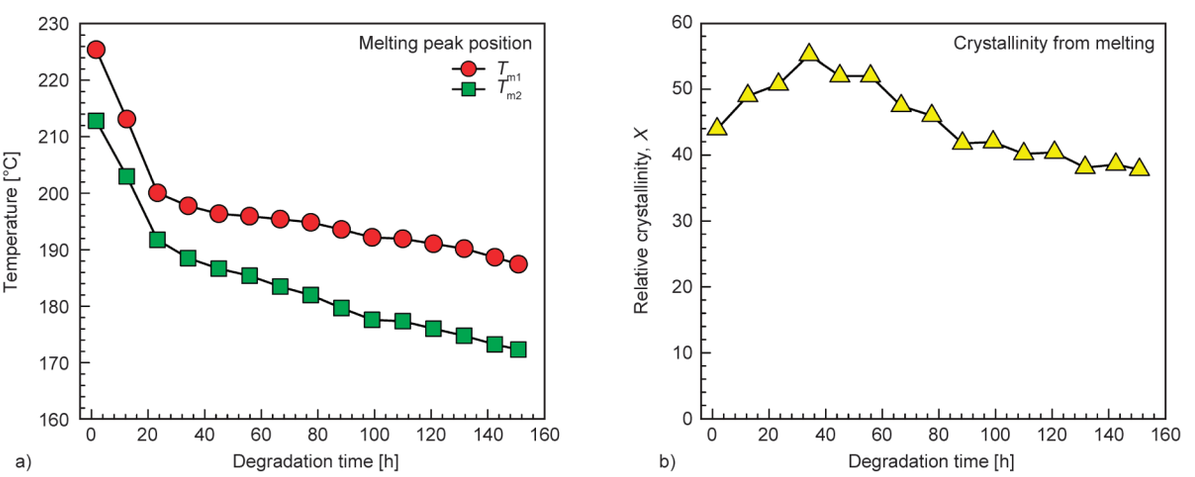


**Figure 14.** DSC results at heating rate 20 °C/min: a) positions of higher and lower melting peaks, b) change in crystallinity derived from melting peaks.

**Table 4.** Positions of melting peaks $T_{m1}$ and $T_{m2}$ and relative crystallinity $X$ from the heating experiment at 20 °C/min as a function of degradation time at 270 °C.

| Time [h] | $T_{m1}$ [°C] | $T_{m2}$ [°C] | $X$ |
|---|---|---|---|
| 1.67 | 225.4 | 212.8 | 43.93 |
| 12.50 | 213.1 | 203.0 | 48.99 |
| 23.33 | 200.1 | 191.8 | 50.73 |
| 34.17 | 197.8 | 188.5 | 55.19 |
| 45.00 | 196.4 | 186.7 | 52.02 |
| 55.83 | 195.9 | 185.4 | 52.00 |
| 66.67 | 195.4 | 183.5 | 47.46 |
| 77.50 | 194.8 | 182.0 | 45.97 |
| 88.33 | 193.6 | 179.7 | 41.78 |
| 99.17 | 192.2 | 177.6 | 41.96 |
| 110.00 | 191.9 | 177.3 | 40.17 |
| 120.83 | 191.1 | 176.0 | 40.39 |
| 131.67 | 190.2 | 174.8 | 38.10 |
| 142.50 | 188.7 | 173.3 | 38.55 |
| 150.83 | 187.4 | 172.3 | 37.78 |

88.33 to 150.83 h, the decrease in crystallinity is relatively moderate. The increase and decrease in crystallinity follow perfectly the trend illustrated by Wang *et al*. [29].

Rabello and White [26] observed similar behaviour for photodegraded polypropylene. After 3 weeks of photodegradation, they observed increased crystallization kinetics followed by a steady decrease until the end of the experiment (24 weeks).

Fraïsse *et al*. [32] reported a decrease in crystallization kinetics for poly(ethylene oxide) samples exposed to thermo-ageing using photo DSC at 55 °C. The half time of crystallization for photo-oxidation of PEO at 15 °C has increased from 105 to 345 s. For the thermo-oxidation experiment at 75 °C, the time of crystallization increased from 101 to 266 s after thermo-oxidation for 1200 s, *i.e.*, the crystallization kinetics became relatively slower.

Overall, thermal degradation exerts a significant influence on the crystallization kinetics of PBT. Its inherent crystallization behaviour is notably altered as it undergoes thermal degradation, characterized by chain scission, cross-linking, and molecular weight reduction. The variations in molecular weight distribution, chain mobility, and polymer conformation introduced by degradation intricately impact the nucleation and growth processes central to crystallization kinetics. These alterations in polymer structure can lead to changes in crystallization temperature, crystallinity, and growth rates, necessitating a comprehensive analysis to unravel the underlying mechanisms. Next, we will illustrate the effects of thermal degradation on the melting temperatures of PBT and clarify the appearance of double melting points that is associated with lamellar thickness.

The presence of two melting peaks (in the DSC experiment) suggests that the situation is more complicated, *i.e.*, the presence of thicker and thinner lamellae and the decrease in thickness of both during the degradation [43]. Many researchers have described the long period and lamellar thickness calculation from SAXS data [44–49].

Crystalline structure analysis was undertaken using SAXS, and the long period involved was determined using Equation (5) [49]:

$$L = \frac{2\pi}{q_{max}} \tag{5}$$

where $L$ is the long period related to the scattering peak position, and $q_{max}$ is the value of scattering vector at maximum.

A clear reduction in the long period is observed due to irradiation. The initial sample exhibited a long period of $L$ = 12.31 nm, whereas the sample subjected to thermal decomposition at degradation time of 30 h demonstrated a long period of $L$ = 10.91 nm (see Table 5).

The effect of thermal degradation on the lamellar thickness can be noted clearly with the help of Gibbs-Thomson equation. The equation calculates the change in melting point with lamellar thickness. It assumes that the crystal sizes $a$ and $b$ with thickness $l$; we can calculate the melting temperature ($T_m$) by Equation (6) [48]:

$$T_m(l) = T_m^0\left(1 - \frac{2}{\Delta h}\left(\frac{\sigma}{a} + \frac{\sigma}{b} + \frac{\sigma_e}{l}\right)\right) \tag{6}$$

where $T_m^0$ is the equilibrium melting point, $\Delta h$ is the heat of fusion, σ is the surface free energy, and $\sigma_e$ is the end surface free energy. Equation (6) can be modified into (Equation (7)):

**Table 5.** SAXS results: peak position $q_m$ [nm$^{-1}$] and long period $L$ [nm] as a function of degradation time at 270 °C.

| Time [h] | $q_{max}$ [nm$^{-1}$] | $L$ [nm] |
|---|---|---|
| 0.83 | 0.5179 | 12.13 |
| 23.33 | 0.5605 | 11.21 |
| 30.00 | 0.5761 | 10.91 |

$$T_m(l) = T_m^0 - \frac{C}{l} \quad \text{where} \quad C = \frac{2\sigma_e T_m^0}{\Delta h} \tag{7}$$

In the case of a particular material, it becomes feasible to assess the reduction in lamellar thickness by gauging the decline in melting point (Equation (8)):

$$\frac{l_2}{l_1} = \frac{T_m^0 - T_{m1}(l)}{T_m^0 - T_{m2}(l)} \tag{8}$$

where $l_1$ is the original lamellar thickness with original melting point $T_{m1}$ and $l_2$ is a new thickness after the treatment with new melting point $T_{m2}$.

These data agree well with the literature presented, *e.g.* by Hsiao *et al*. [50], who observed the peak position of intensity when $q$ was in the range 0.4 to 0.5 nm$^{-1}$ for pristine PBT.

The surface free energy (σ) probably remains constant under the long degradation time, and that leads to a decrease in the melting temperature ($T_m$).

One-dimensional correlation function can be calculated by using the Equation (9) [51]:

$$\gamma(r) = \frac{2\pi^2}{Q}\int_0^\infty I(q)q^2\cos(qr)\,\mathrm{d}q \tag{9}$$

where $r$ is the direction perpendicular to the surfaces of the lamellae, along which the electron density is measured. $\gamma(0) = 1$ at $r = 0$; $Q$ is the scattering invariant (Equation (10)):

$$Q = \frac{1}{2\pi^2}\int_0^\infty I(q)q^2\,\mathrm{d}q \tag{10}$$

Finally, the volume fraction of the crystallites $\phi_c$, by Equation (11):

$$Q = \phi_c(1-\phi_c)\Delta\rho_e^2 \tag{11}$$

where $\Delta\rho_e$ denotes the electron density contrast between the crystalline and amorphous layers.

Both the long period ($L_p$) and lamellar thickness ($l_c$) decrease during the degradation. The long-period values obtained by two independent methods (Bragg's equation *vs*. one-dimensional correlation function) have slightly different values but reveal the same decreasing trend with progressing degradation. The 'one-dimensional correlation function' method also has the advantage of getting the lamellar thickness.

Our data are not very far from Hsiao *et al*. [50], who found long periods in the range 10–14 nm for pure PBT. The higher numbers correspond to higher crystallization temperatures. They observed slightly higher lamellar thickness (around 5 to 8 nm). They have performed isothermal crystallization at elevated temperatures, some of them quite close to $T_m$, while our samples crystallized during quite rapid nonisothermal cooling at rate 20 °C. Hence, our smaller lamellar thickness is not that surprising.

We have observed a decrease in melting point during the degradation. Based on the Gibbs-Thomson equation, we could assume that the lamellar thickness decreases during degradation. This was confirmed by SAXS measurement.

Initially, there is mainly one peak (even though the second peak is also present). In the later part of degradation, the presence of two peaks is evident and might mean the presence of lamellae with two different thicknesses.

The $T_{m1}$ and $T_{m2}$ are still moving towards the lower temperatures, so we can assume a moderate decrease in both lamellar thicknesses. The results from SAXS (see Figures 15 and 16 and Table 5) confirmed a decrease in long-period $L$ that comprises the lamellar thickness plus the amorphous layer's thickness. The data from SAXS indicate a decrease in lamellar thickness during the degradation [52].

## 4. Conclusions

The results reveal a substantial shift in $T_c$, indicating a significant alteration in the crystallization temperature of PBT. Throughout the experiment, the $T_c$ shifts from an initial value of 193 °C to a final value of 133 °C, marking a notable 60 °C decrease. This shift progresses through three distinct periods: an initial increase in $T_c$, an intermediate stage characterized by a steep decrease, and a late-stage degradation period with rather moderate decline. Crystallinity and crystallization kinetics exhibit a similar trend, with an increase followed by a steep decrease during the intermediate degradation period and a subsequent moderate decrease in the late-stage period. Additionally, the study identifies the presence of two melting peaks in the DSC data, suggesting the presence of two distinct lamellar thicknesses. These peaks experience a decrease in melting point ($T_m$), where the higher melting point $T_{m1}$ changed during degradation from 225 to 187 °C (a 38 °C decrease) while the lower melting point $T_{m2}$ changed during degradation from 213 to 172 °C (a 41 °C decrease). While the $T_m$ changed about 40 °C towards lower temperatures, the $T_c$ decreased much more (60 °C). Since these two temperatures usually are very much

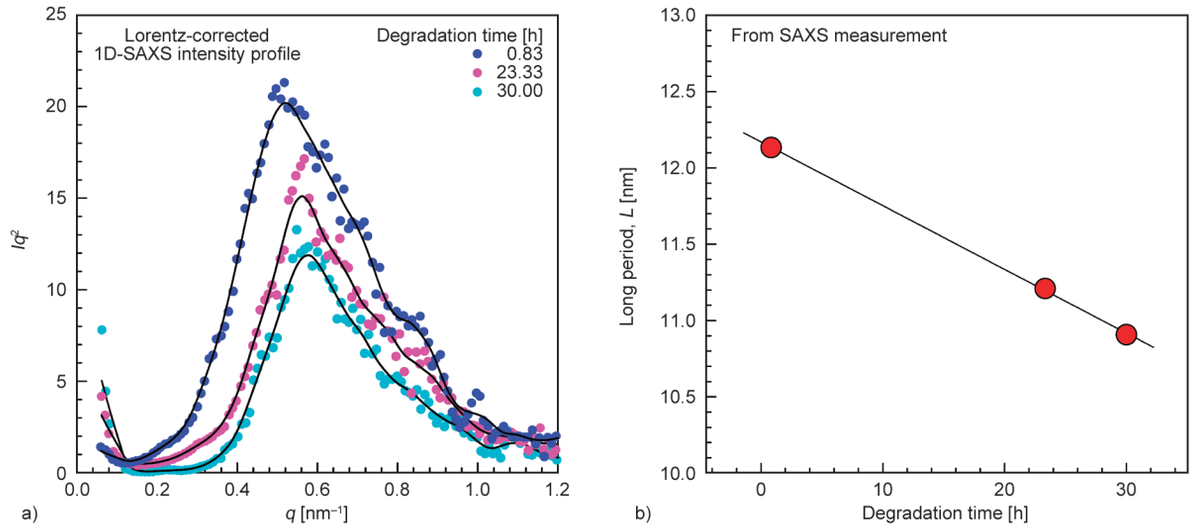


**Figure 15.** The influence of degradation on small angle X-ray scattering data. a) Lorentz-corrected 1D-SAXS intensity profiles, b) change in long period L during the degradation.

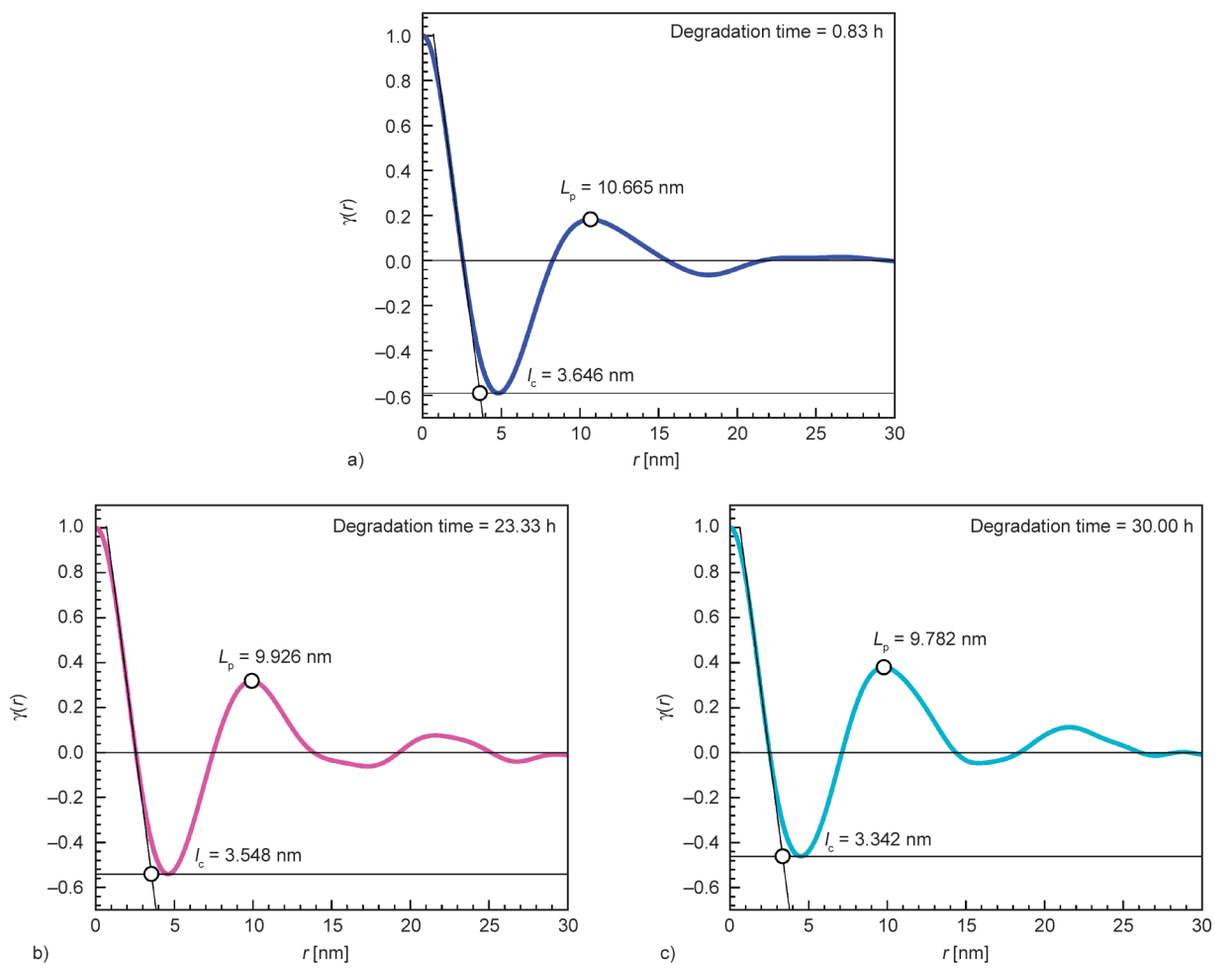


**Figure 16.** SAXS one dimensional correlation function for PBT after degradation a) 0.83 h, b) 23.33 h and c) 30.00 h. $L_p$ is long period, and $l_c$ is lamellar thickness.

connected to each other, the change in $T_c$ contains information about the ability of molecules to crystallize after degradation. Apparently, the ability of molecules to crystallize is much lower after degradation, which was also quantitatively confirmed by slower crystallization kinetics (besides much lower $T_c$). Small-angle X-ray scattering (SAXS) analysis further supports the degradation-induced changes, revealing

a decrease in the long period and lamellar thickness. Our work effectively illustrates the influence of the degradation stages on nonisothermal crystallization, highlighting the gradual decrease in $T_c$, peak height, crystallinity, and crystallization kinetics during the late-stage degradation. Our research emphasizes the complex nature of the crystallization behaviour of PBT under thermal degradation, reflecting the interplay of factors such as lamellar thickness and molecular weight. The study's comprehensive analysis and comparison with related research contribute to the broader understanding of polymer degradation and its impact on crystallization. Further investigations into these changes' intricate mechanisms could offer valuable insights into tailoring polymer properties for specific applications, fostering advancements in polymer engineering and materials science.

## Acknowledgements

The University of Tomas Bata in Zlin funded this research through its internal grant agency (IGA/FT/2023/008).

## References

[1] Wang M., Guo L., Sun H.: Manufacture of biomaterials. Elsevier, Oxford (2019).

[2] Parra D. F., Fusaro J., Gaboardi F., Rosa D. S.: Influence of poly(ethylene glycol) on the thermal, mechanical, morphological, physical-chemical and biodegradation properties of poly(3-hydroxybutyrate). Polymer Degradation and Stability, **91**, 1954–1959 (2006). https://doi.org/10.1016/j.polymdegradstab.2006.02.008

[3] Huang J., Wang J., Qiu Y., Wu D.: Mechanical properties of thermoplastic polyester elastomer controlled by blending with poly(butylene terephthalate). Polymer Testing, **55**, 152–159 (2016). https://doi.org/10.1016/j.polymertesting.2016.08.020

[4] Díaz A., Katsarava R., Puiggalí J.: Synthesis, properties and applications of biodegradable polymers derived from diols and dicarboxylic acids: From polyesters to poly(ester amide)s. International Journal of Molecular Sciences, **15**, 7064–7123 (2014). https://doi.org/10.3390/ijms15057064

[5] Dong Y., Yang H., Wu Y., Zou Y., Yuan J., Cui C., Li Y.: Towards improved efficiency of polymer solar cells *via* chlorination of a benzo[1,2-b:4,5-b′]dithiophene based polymer donor. Journal of Materials Chemistry A, **7**, 2261–2267 (2019). https://doi.org/10.1039/C8TA10923K

[6] Hwang H., Sin D. H., Park C., Cho K.: Ternary organic solar cells based on a wide-bandgap polymer with enhanced power conversion efficiencies. Scientific Reports, **9**, 12081 (2019). https://doi.org/10.1038/s41598-019-48306-x

[7] Nasybulin E., Feinstein J., Cox M., Kymissis I., Levon K.: Electrochemically prepared polymer solar cell by three-layer deposition of poly(3,4-ethylenedioxythiophene)/poly(2,2′-bithiophene)/fullerene (PEDOT/PBT/$C_{60}$). Polymer, **52**, 3627–3632 (2011). https://doi.org/10.1016/j.polymer.2011.06.020

[8] Bikiaris D. N., Karayannidis G. P.: Effect of carboxylic end groups on thermooxidative stability of PET and PBT. Polymer Degradation and Stability, **63**, 213–218 (1999). https://doi.org/10.1016/S0141-3910(98)00094-9

[9] Murmu U. K., Adhikari J., Naskar A., Dey D., Roy A., Ghosh A., Ghosh M.: Encyclopedia of materials: Plastics and polymers. Elsevier, Oxford (2022).

[10] Payal R. S., Sommer J-U.: Crystallization of polymers under the influence of an external force field. Polymers, **13**, 2078 (2021). https://doi.org/10.3390/polym13132078

[11] Samperi F., Puglisi C., Alicata R., Montaudo G.: Thermal degradation of poly(butylene terephthalate) at the processing temperature. Polymer Degradation and Stability, **83**, 11–17 (2004). https://doi.org/10.1016/S0141-3910(03)00167-8

[12] McNeill I. C., Bounekhel M.: Thermal degradation studies of terephthalate polyesters: 1. Poly(alkylene terephthalates). Polymer Degradation and Stability, **34**, 187–204 (1991). https://doi.org/10.1016/0141-3910(91)90119-C

[13] Lum R. M.: Thermal decomposition of poly(butylene terephthalate). Journal of Polymer Science Part A: Polymer Chemistry, **17**, 203–213 (1979). https://doi.org/10.1002/pol.1979.170170120

[14] Passalacqua V., Pilati F., Zamboni V., Fortunato B., Manaresi P.: Thermal degradation of poly(butylene terephthalate). Polymer, **17**, 1044–1048 (1976). https://doi.org/10.1016/0032-3861(76)90004-5

[15] Hage E., Hale W., Keskkula H., Paul D. R.: Impact modification of poly(butylene terephthalate) by ABS materials. Polymer, **38**, 3237–3250 (1997). https://doi.org/10.1016/S0032-3861(96)00879-8

[16] Edge M., Hayes M., Mohammadian M., Allen N. S., Jewitt T. S., Brems K., Jones K.: Aspects of poly(ethylene terephthalate) degradation for archival life and environmental degradation. Polymer Degradation and Stability, **32**, 131–153 (1991). https://doi.org/10.1016/0141-3910(91)90047-U

[17] Montaudo G., Puglisi C., Samperi F.: Primary thermal degradation mechanisms of PET and PBT. Polymer Degradation and Stability, **42**, 13–28 (1993). https://doi.org/10.1016/0141-3910(93)90021-A

[18] Loyer C., Régnier G., Duval V., Ould Y., Richaud E.: PBT plasticity loss induced by oxidative and hydrolysis ageing. Polymer Degradation and Stability, **181**, 109368 (2020). https://doi.org/10.1016/j.polymdegradstab.2020.109368

[19] Loyer C., Ferreira P., Marijon J-B., Michel V., Régnier G., Vera J., Duval V., Richaud E.: Embrittlement of polybutylene terephthalate induced by injection molding. Polymer Degradation and Stability, **196**, 109843 (2022). https://doi.org/10.1016/j.polymdegradstab.2022.109843

[20] Rangari D., Vasanthan N.: Study of strain-induced crystallization and enzymatic degradation of drawn poly(L-lactic acid) (PLLA) films. Macromolecules, **45**, 7397–7403 (2012). https://doi.org/10.1021/ma301482j

[21] Hoffman J. D., Miller R. L.: Test of the reptation concept: Crystal growth rate as a function of molecular weight in polyethylene crystallized from the melt. Macromolecules, **21**, 3038–3051 (1988). https://doi.org/10.1021/ma00188a024

[22] Avrami M.: Kinetics of phase change. I General theory. The Journal of Chemical Physics, **7**, 1103 (1939). https://doi.org/10.1063/1.1750380

[23] Ergoz E., Fatou J. G., Mandelkern L.: Molecular weight dependence of the crystallization kinetics of linear polyethylene. I. Experimental results. Macromolecules, **5**, 147–157 (1972). https://doi.org/10.1021/Ma60026a011

[24] Chen H. L., Li L. J., Ou-Yang W. C., Hwang J. C., Wong W. Y.: Spherulitic crystallization behavior of poly(ε-caprolactone) with a wide range of molecular weight. Macromolecules, **30**, 1718–1722 (1997). https://doi.org/10.1021/Ma960673v

[25] Chen X., Hou G., Chen Y., Yang K., Dong Y., Zhou H.: Effect of molecular weight on crystallization, melting behavior and morphology of poly(trimethylene terephalate). Polymer Testing, **26**, 144–153 (2007). https://doi.org/10.1016/j.polymertesting.2006.08.011

[26] Rabello M. S., White J. R.: Crystallization and melting behaviour of photodegraded polypropylene – II. Recrystallization of degraded molecules. Polymer, **38**, 6389–6399 (1997). https://doi.org/10.1016/S0032-3861(97)00214-0

[27] Muthuraj R., Misra M., Mohanty A. K.: Hydrolytic degradation of biodegradable polyesters under simulated environmental conditions. Journal of Applied Polymer Science, **132**, 42189 (2015). https://doi.org/10.1002/app.42189

[28] Avella M., Dell'Erba R., Martuscelli E.: Fiber reinforced polypropylene: Influence of iPP molecular weight on morphology, crystallization, and thermal and mechanical properties. Polymer Composites, **17**, 288–299 (1996). https://doi.org/10.1002/Pc.10613

[29] Wang X-S., Yan D., Tian G-H., Li X-G.: Effect of molecular weight on crystallization and melting of poly (trimethylene terephthalate). 1: Isothermal and dynamic crystallization. Polymer Engineering and Science, **41**, 1655–1664 (2001). https://doi.org/10.1002/Pen.10863

[30] Xu J., Shi W.: Synthesis and crystallization kinetics of silsesquioxane-based hybrid star poly(ε-caprolactone). Polymer, **47**, 5161–5173 (2006). https://doi.org/10.1016/j.polymer.2006.04.062

[31] Seo J., Zhang X. S., Schaake R. P., Rhoades A. M., Colby R. H.: Dual nakamura model for primary and secondary crystallization applied to nonisothermal crystallization of poly(ether ether ketone). Polymer Engineering and Science, **61**, 2416–2426 (2021). https://doi.org/10.1002/pen.25767

[32] Fraïsse F., Nedelec J-M., Grolier J. P. E., Baba M.: Isothermal crystallization kinetics of *in situ* photo and thermo aged poly(ethylene oxide) using photoDSC. Physical Chemistry Chemical Physics, **9**, 2137–2141 (2007). https://doi.org/10.1039/B618701c

[33] Tsuji H., Shimizu K., Sato Y.: Hydrolytic degradation of poly(L-lactic acid): Combined effects of UV treatment and crystallization. Journal of Applied Polymer Science, **125**, 2394–2406 (2012). https://doi.org/10.1002/app.36498

[34] Nakamura K., Katayama K., Amano T.: Some aspects of nonisothermal crystallization of polymers. II. Consideration of the isokinetic condition. Journal of Applied Polymer Science, **17**, 1031–1041 (1973). https://doi.org/10.1002/app.1973.070170404

[35] Pospíšil L., Rybníkař F.: Crystallization of controlled rheology type polypropylene. Polymer, **31**, 476–480 (1990). https://doi.org/10.1016/0032-3861(90)90388-F

[36] Ou-Yang W-C., Li L-J., Chen H-L., Hwang J. C.: Bulk crystallization behavior of poly(ε-caprolactone) with a wide range of molecular weight. Polymer Journal, **29**, 889–893 (1997). https://doi.org/10.1295/polymj.29.889

[37] Wu T., Yu L., Cao Y., Yang F., Xiang M.: Effect of molecular weight distribution on rheological, crystallization and mechanical properties of polyethylene-100 pipe resins. Journal of Polymer Research, **20**, 271 (2013). https://doi.org/10.1007/S10965-013-0271-9

[38] Galante M. J., Mandelkern L., Alamo R. G., Lehtinen A., Paukkeri R.: Crystallization kinetics of metallocene type polypropylenes: Influence of molecular weight and comparison with Ziegler-Natta type systems. Journal of Thermal Analysis, **47**, 913–929 (1996). https://doi.org/10.1007/Bf01979439

[39] Isayev A. I., Catignani B. F.: Crystallization and microstructure in quenched slabs of various molecular weight polypropylenes. Polymer Engineering and Science, **37**, 1526–1539 (1997). https://doi.org/10.1002/Pen.11801

[40] Ozawa T.: Kinetics of non-isothermal crystallization. Polymer, **12**, 150–158 (1971). https://doi.org/10.1016/0032-3861(71)90041-3

[41] Rodriguez E. J., Marcos B., Huneault M. A.: Hydrolysis of polylactide in aqueous media. Journal of Applied Polymer Science, **133**, 44152 (2016). https://doi.org/10.1002/app.44152

[42] Saha S. K., Tsuji H.: Effects of rapid crystallization on hydrolytic degradation and mechanical properties of poly(L-lactide-*co*-ε-caprolactone). Reactive and Functional Polymers, **66**, 1362–1372 (2006). https://doi.org/10.1016/j.reactfunctpolym.2006.03.020

[43] Ren Y., Zou H., Wang S., Liu J., Gao D., Wu C., Zhang S.: Effect of annealing on microstructure and tensile properties of polypropylene cast film. Colloid and Polymer Science, **296**, 41–51 (2018). https://doi.org/10.1007/s00396-017-4220-8

[44] Housmans J-W., Gahleitner M., Peters G. W. M., Meijer H. E. H.: Structure-property relations in molded, nucleated isotactic polypropylene. Polymer, **50**, 2304–2319 (2009). https://doi.org/10.1016/j.polymer.2009.02.050

[45] Janicek M., Cermak R., Obadal M., Piel C., Ponizil P.: Ethylene copolymers with crystallizable side chains. Macromolecules, **44**, 6759–6766 (2011). https://doi.org/10.1021/ma201017m

[46] Al Mamun, Rahman S. M. M., Aiken C.: Influences of the chemical defects on the crystal thickness and their melting of isothermally crystallized isotactic polypropylene. Journal of Polymer Research, **24**, 145 (2017). https://doi.org/10.1007/s10965-017-1304-6

[47] Picu R. C., Osta A. R.: Elastic constants of lamellar and interlamellar regions in and mesomorphic isotactic polypropylene by AFM indentation. Journal of Applied Polymer Science, **133**, 43649 (2016). https://doi.org/10.1002/app.43649

[48] Svoboda P., Trivedi K., Stoklasa K., Svobodova D., Ougizawa T.: Study of crystallization behaviour of electron beam irradiated polypropylene and high-density polyethylene. Royal Society Open Science, **8**, 202250 (2021). https://doi.org/10.1098/rsos.202250

[49] Liu X., Dai K., Hao X., Zheng G., Liu C., Schubert D. W., Shen C.: Crystalline structure of injection molded β-isotactic polypropylene: Analysis of the oriented shear zone. Industrial and Engineering Chemistry Research, **52**, 11996–12002 (2013). https://doi.org/10.1021/ie401162c

[50] Hsiao B. S., Wang Z-G., Yeh F., Gao Y., Sheth K. C.: Time-resolved X-ray studies of structure development in poly(butylene terephthalate) during isothermal crystallization. Polymer, **40**, 3515–3523 (1999). https://doi.org/10.1016/S0032-3861(98)00573-4

[51] Sun Y-S.: Temperature-resolved SAXS studies of morphological changes in melt-crystallized poly(hexamethylene terephthalate) and its melting upon heating. Polymer, **47**, 8032–8043 (2006). https://doi.org/10.1016/j.polymer.2006.09.003

[52] Mani M. R., Chellaswamy R., Marathe Y. N., Pillai V. K.: New understanding on regulating the crystallization and morphology of the beta-polymorph of isotactic polypropylene based on carboxylate-alumoxane nucleating agents. Macromolecules, **49**, 2197–2205 (2016). https://doi.org/10.1021/acs.macromol.5b02466